

# Supplementary information for “Performance of wave function and Green’s function methods for non-equilibrium many-body dynamics”

Cian C. Reeves,<sup>1</sup> Gaurav Harsha,<sup>2</sup> Avijit Shee,<sup>3</sup> Yuanran Zhu,<sup>4</sup> Chao Yang,<sup>4</sup> K Birgitta Whaley,<sup>3,5</sup> Dominika Zgid,<sup>2,6</sup> and Vojtěch Vlček<sup>7,8</sup>

<sup>1</sup>*Department of Physics, University of California, Santa Barbara, Santa Barbara, CA 93117*

<sup>2</sup>*Department of Chemistry, University of Michigan, Ann Arbor, Michigan 48109, USA*

<sup>3</sup>*Department of Chemistry, University of California, Berkeley, USA*

<sup>4</sup>*Applied Mathematics and Computational Research Division,*

*Lawrence Berkeley National Laboratory, Berkeley, CA 94720, USA*

<sup>5</sup>*Berkeley Center for Quantum Information and Computation, Berkeley*

<sup>6</sup>*Department of Physics, University of Michigan, Ann Arbor, Michigan 48109, USA*

<sup>7</sup>*Department of Chemistry and Biochemistry, University of California, Santa Barbara, Santa Barbara, CA 93117*

<sup>8</sup>*Department of Materials, University of California, Santa Barbara, Santa Barbara, CA 93117*

(Dated: May 14, 2024)

## I. THEORY

### A. Time-dependent configuration interaction

Configuration Interaction (CI) is a wave function-based many-body method, where the exact correlated wave function ( $|\Psi\rangle$ ) is expressed in terms of the ground and excited Slater determinants ( $|\Phi_I\rangle$ ):  $|\Psi\rangle = \sum_I |\Phi_I\rangle$ , where  $I$  stands for various electronic configurations. When ( $|\Psi\rangle$ ) is plugged into the time-dependent Schrödinger equation, we obtain the following equations of motion for the  $C_I$ s:

$$i\frac{\partial C_I}{\partial t} = \sum_J H_{IJ}(t)C_J \quad (1)$$

The solution of Eqn. (1) can be written as:

$$C_I(t_n) = \sum_J U_{IJ}(t_n, t_0)C_J(t_0); \quad U_{IJ}(t_n, t_0) = \mathcal{T}\{\exp[-i \int_{t_0}^{t_n} dt H_{IJ}(t)]\} \quad (2)$$

In order to evaluate  $U_{IJ}(t_n, t_0)$  numerically we required two components: implementation of the time-ordering and the evaluation of the exponential of a large matrix. In Fig. S1 we have shown the numerical implementation of the time-ordering. We first break the time interval  $[t_0, t_n]$  into many slices and choose a fixed time-ordering:  $t_0 \leq t_1 \leq t_2 \leq \dots \leq t_{n-1} \leq t_n$ . Also, we assume that the Hamiltonian is piecewise constant within a time-interval:  $\hat{H}(t) = \hat{H}(t_p) \forall t_p < t \leq t_{p+1}$ .

Therefore, Eq. 2 can be written as:

$$\mathbf{C}(t_n) = \mathcal{T}\{e^{-i\hat{H}(t_{n-1})\Delta t} \dots e^{-i\hat{H}(t_1)\Delta t} e^{-i\hat{H}(t_0)\Delta t}\} \mathbf{C}(t_0) \quad (3)$$

where we have used the fact that within time-ordering the operators commute.

To evaluate the exponential of a large matrix (time-independent) we first make a polynomial approximation of the time-evolution operator:

$$C_I(t + \tau) = \sum_J e^{-iH_{IJ}\tau} C_J(t) \quad (4)$$

$$\approx \sum_J \sum_{k=1}^p \frac{(-i\tau)^k}{k!} H_{IJ}^k C_J(t) \quad (5)$$

$$\approx \sum_{k=1}^p \frac{(-i\tau)^k}{k!} a_I^k(t) \quad (6)$$

where,  $a_I^k(t)$ s are

$$a_I^k(t) = H_{IJ} a_J^{k-1}(t); \quad a_J^0(t) = C_J(t) \quad (7)$$

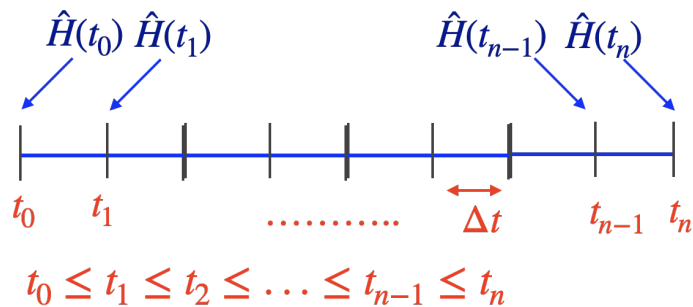


FIG. S1: Numerical implementation of time-ordering

$a^k$  vectors form a subspace  $A_k = [a^0 a^1 \dots a^k]$ . If we employ the Lanczos procedure to generate the subspace, the Hamiltonian becomes tridiagonal within that subspace. We can do a basis transformation by using the  $A_k$  transformation matrix to generate a reduced dimensional ( $p \times p$ ) time-evolution equation [1]. The solution of those equations can be written down as:

$$\mathbf{d}(t + \tau) = e^{-iH_p \tau} \mathbf{d}(t) \quad (8)$$

Here,  $\mathbf{d}(t) = A_k \mathbf{C}(t)$  is a ( $p \times 1$ ) vector. Finally,  $\mathbf{C}(t + \tau)$ s can be obtained as:

$$\mathbf{C}(t + \tau) = A_k \mathbf{d}(t + \tau) \quad (9)$$

However, the tridiagonal  $H_p$  provides a time-local description of the propagator, which becomes unsuitable after a certain time step,  $\Delta t^{max}$ . This limit can be exactly evaluated [2] by analyzing the accuracy of the series expansion up to a threshold  $\epsilon$  in Eq. 6 for a value of  $p$ , that is the dimension of the Krylov space. Once, that time limit is reached, we evaluate the CI coefficients at that time-step from Eq. (9), and from there we construct a new subspace time evolution operator,  $U_p$ . For the time-dependent Hamiltonian, we evaluate the Hamiltonian at  $(t + \Delta t^{max})$  and build  $U_p$  based on that.

*Implementaion details* The one- and two-electron integrals for all calculations were prepared using PySCF. [3, 4] The time-propagation grid in this method is generated by the Lanczos technique, which is typically quite sparse.

## B. Time-dependent coupled cluster

Coupled cluster (CC) theory [5, 6] is widely accepted as one of the most accurate wavefunction methods for weakly correlated systems. This is has led to generalizations of traditional ground-state CC to time-dependent methods. In this paper, we use the time-dependent CC (TDCC) theory formulated by Arponen, [7] where we first define the time-dependent action integral using the non-Hermitian CC ansatz, such that we have

$$S = \int dt \mathcal{L}(t) = \int dt \langle \Phi | (1 + Z(t)) e^{-T(t)} \left( i \frac{\partial}{\partial t} - H(t) \right) e^{T(t)} | \Phi \rangle. \quad (10)$$

Here,  $|\Phi\rangle$  is a Hartree-Fock Slater determinant, while the cluster operators  $T(t)$  and  $Z(t)$  are defined using particle-hole creation and annihilation operators, respectively,

$$T(t) = \sum_{ia} \tau_i^a c_a^\dagger c_i + \frac{1}{4} \sum_{ijab} \tau_{ij}^{ab} c_a^\dagger c_b^\dagger c_j c_i + \dots, \quad (11a)$$

$$Z(t) = \sum_{ia} z_i^a c_i^\dagger c_a + \frac{1}{4} \sum_{ijab} z_{ij}^{ab} c_i^\dagger c_j^\dagger c_b c_a + \dots. \quad (11b)$$

We have adopted chemist's notation for orbital index, i.e., indices  $i, j, k, l, \dots$  denote occupied orbitals, while  $a, b, c, d, \dots$  denote unoccupied (or virtual) orbitals, and finally,  $p, q, r, s, \dots$  are used as general labels. When the cluster operators are expanded to all orders in particle-hole excitation rank, the CC ansatz provides an exact parametrization of the many-body wave function. However, for practical implementations,  $T$  and  $Z$  are truncated to single and double excitation, resulting in the well known CCSD approximation.

The evolution equations for  $\tau$  and  $z$  amplitudes are found by making the action  $S$  stationary with respect to variations in  $T$  and  $Z$ . In principle, the action also depends on the molecular orbital basis used to construct the

mean-field reference  $|\Phi\rangle$ , such a time-dependent orbital optimization is not considered here. In other words,  $|\Phi\rangle$  is considered to be time-independent and all the time-dependence is incorporated by the CC amplitudes.

Considering the compact notation  $T = \sum_{\mu} \tau_{\mu} \gamma_{\mu}^{\dagger}$  and  $Z = \sum_{\mu} z_{\mu} \gamma_{\mu}$ , where  $\gamma_{\mu}^{\dagger}$  and  $\gamma_{\mu}$  represent particle-hole excitation and de-excitation operators, the Lagrangian can be simplified as

$$\mathcal{L}(t) = i \sum_{\mu} z_{\mu} \frac{\partial \tau_{\mu}}{\partial t} \langle \Phi | \gamma_{\mu} \gamma_{\mu}^{\dagger} | \Phi \rangle - \langle \Phi | (1 + Z) e^{-T} H e^T | \Phi \rangle. \quad (12)$$

The associated Euler-Lagrange equations are our desired evolution equations. For the  $\tau$ -amplitudes, we have

$$\frac{\partial \mathcal{L}}{\partial z_{\mu}} = 0 \Rightarrow i \langle \Phi | \gamma_{\mu} \gamma_{\mu}^{\dagger} | \Phi \rangle \frac{\partial \tau_{\mu}}{\partial t} = \langle \Phi | \gamma_{\mu} e^{-T} H e^T | \Phi \rangle, \quad (13)$$

while for  $z$ -amplitudes, one obtains

$$\frac{d}{dt} \left( \frac{\partial \mathcal{L}}{\partial (\partial \tau_{\mu} / \partial t)} \right) = \frac{\partial \mathcal{L}}{\partial \tau_{\mu}} \Rightarrow i \langle \Phi | \gamma_{\mu} \gamma_{\mu}^{\dagger} | \Phi \rangle \frac{\partial z_{\mu}}{\partial t} = - \langle \Phi | (1 + Z) e^{-T} [H, \gamma_{\mu}^{\dagger}] e^T | \Phi \rangle. \quad (14)$$

Explicit expressions for these equations contain a lot of terms, and were derived with the help of *drudge* symbolic algebra manipulator. [8] Starting from a known initial condition for the CC amplitudes, these equations can be integrated to obtain the time-dependent CC wave functions. Unlike traditional ground-state CC, where orbitals and amplitudes can be chosen to be real-valued, in TDCC, the CC amplitudes develop a complex part as we evolve in time.

In CC theory, observable quantities are defined as asymmetric expectation values, i.e., for an operator  $A$ , we have

$$\langle A \rangle_{CC} = \langle \Phi | (1 + Z) e^{-T} A e^T | \Phi \rangle. \quad (15)$$

Due to the asymmetric nature of this expression, combined with the fact that the  $T$  and  $Z$  amplitudes are complex numbers, CC estimates for an observable develop a non-physical complex value. While there may be different ways to address this problem, we adopt the simplest solution by dropping the imaginary part. It is a general observation that when the CC ansatz is a good approximation, these imaginary components remain small and can be ignored for practical purpose. On the other hand, when multi-reference character in the time-dependent wave function grows, and CC starts to break down, there is a corresponding increase in the magnitude of both real and imaginary terms in the CC amplitudes. As a result, CC expectation values return extremely non-physical results; even occupation numbers may become negative or larger than unity. Therefore, tracking the magnitude of CC amplitudes (and in TDCC, also the size of imaginary part) is a well known practical way to predict the effectiveness of the CC ansatz.

*Implementaion details* The one- and two-electron integrals for all calculations were prepared using PySCF. [3, 4] The TD-CC equations for the amplitudes  $t_{\mu}$  and  $z_{\mu}$  are integrated with the Variable-coefficient Ordinary Differential Equation (VODE) solver available in SciPy. [9, 10] The amplitudes are initialized by solving the ground-state coupled cluster equations in the restricted (or symmetry-adapted) formalism.

### C. The Kadanoff-Baym equations

The Kadanoff-Baym equations describe the time evolution of a two-time non-equilibrium GF initially at equilibrium and perturbed by an external field. In this section, we will introduce the KBEs, as well as some of the theory needed to understand their meaning.

When a system initially at thermal equilibrium at inverse temperature  $\beta$  is perturbed by a time-dependent field, the expectation of an operator can be written generally as[11],

$$\langle \hat{A}(t) \rangle = \frac{\text{Tr}[\hat{U}(-i\beta, 0) \hat{U}^{\dagger}(0, t) \hat{A} \hat{U}(t, 0)]}{\text{Tr}[\hat{U}(-i\beta, 0)]} \quad (16)$$

Here, without loss of generality, we assume the time-dependent field is switched on at  $t = t_0 = 0$ . In the above we also have,

$$U(t_2, t_1) = \begin{cases} \mathcal{T} \{ \exp[-i \int_{t_1}^{t_2} dt \mathcal{H}(t)] \} & t_2 > t_1 \\ \bar{\mathcal{T}} \{ \exp[-i \int_{t_1}^{t_2} dt \mathcal{H}(t)] \} & t_2 < t_1, \end{cases} \quad (17)$$

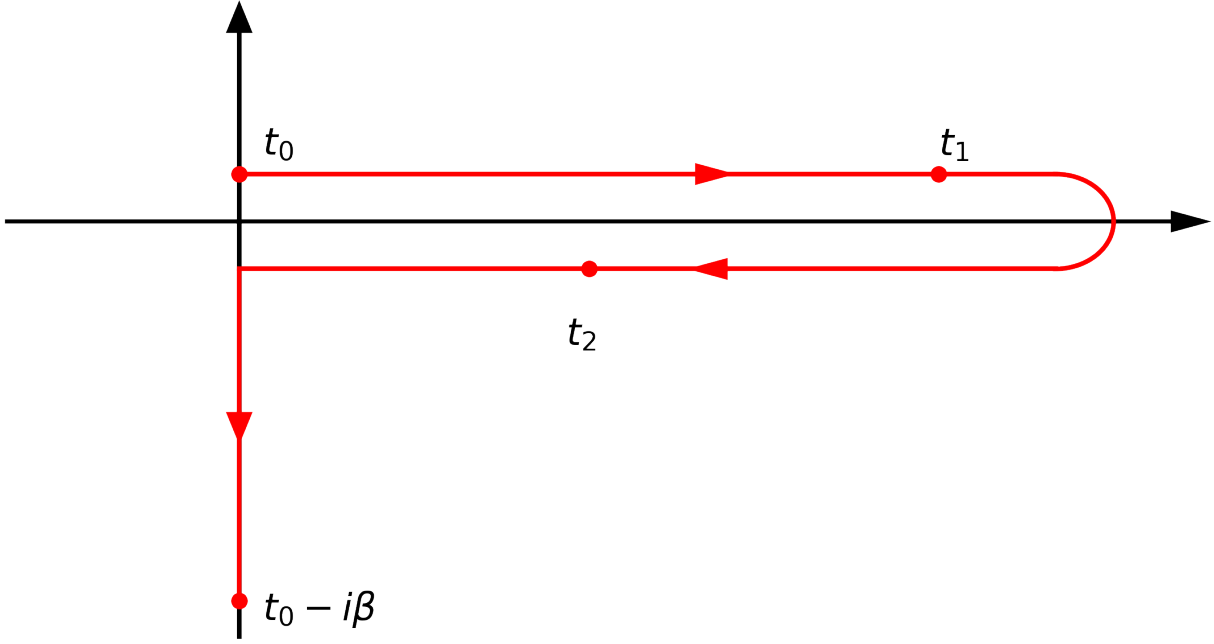


FIG. S2: The Keldysh contour. The contour time ordering operator,  $\mathcal{T}_C$ , places operators from right to left such that their time arguments follow the order of the arrows shown in the contour. The vertical portion of the track relates to the initial preparation while the horizontal portion is related to the non-equilibrium evolution of the operator.

where  $\mathcal{T}(\bar{\mathcal{T}})$  is the (anti-)time-ordering operator. Finally,

$$U(-i\beta, 0) = \exp(-\beta\mathcal{H}(0)), \quad (18)$$

is the thermal statistical averaging operator for a given inverse temperature  $\beta$ . In the following sections, the finite temperature formalism at a sufficiently low temperature is invoked in preparing the correlated ground state for the KBEs. In contrast, the strictly 0K formalism typically employs adiabatic connection to prepare the correlated quantum state. Within the Keldysh formalism, this product can equivalently be written as an ordered product on the contour shown in Fig. S2. The operator  $\mathcal{T}_C$  in equation (19) denotes the contour ordering and places operators from right to left with time arguments in the order that corresponds to the direction of the arrows appearing in Fig. S2. While the details of the Keldysh formalism are not crucial in this work, we do introduce some common definitions in order to present the Kadanoff-Baym equations for the NEGF. For more information on the Keldysh formalism, we direct the reader to [11–14].

Firstly, in the Keldysh formalism the single particle GF can be written as,

$$G(t_1, t_2) = -i\langle \mathcal{T}_C [c(t_1)c^\dagger(t_2)] \rangle. \quad (19)$$

At inverse temperature  $\beta$  and with  $t_0$  denoting the time at which the system leaves equilibrium,  $t_1$  and  $t_2$  can lie anywhere on the contour shown in Fig. S2. When both time arguments lie on the real axis the lesser and greater GFs are defined as follows,

$$\begin{aligned} G^>(t_1, t_2) &= -i\langle c(t_1)c^\dagger(t_2) \rangle, \\ G^<(t_1, t_2) &= i\langle c^\dagger(t_2)c(t_1) \rangle. \end{aligned} \quad (20)$$

The time ordering operator means the full GF in equation (19) will be given by  $G^>(t_1, t_2)$  when  $t_1$  is later than  $t_2$  and  $G^<(t_1, t_2)$  when  $t_2$  is later than  $t_1$  and both are on the real axis. When one of the time arguments lies on the imaginary axis we have,

$$\begin{aligned} G^\Gamma(-i\tau, t) &= G^>(t_0 - i\tau, t), \\ G^\Lambda(t, -i\tau) &= G^<(t, t_0 - i\tau). \end{aligned} \quad (21)$$

Finally, when both arguments lie on the imaginary axis we are left with the time translation invariant Matsubara GF,

$$iG^M(\tau_1 - \tau_2) = G(t_0 - i\tau_1, t_0 - i\tau_2), \quad (22)$$

which represents the equilibrium GF at a given temperature. The same definitions also exist for the self energy operator. Using these notations the KBEs for time propagation of the NEGF can be written explicitly as,

$$\begin{aligned} [-\partial_\tau - h]G^M(\tau) &= \delta(\tau) + \int_0^\beta d\bar{\tau} \Sigma^M(\tau - \bar{\tau})G^M(\bar{\tau}), \\ i\partial_{t_1}G^\uparrow(t_1, -i\tau) &= h^{\text{HF}}(t_1)G^\uparrow(t_1, -i\tau) + I^\uparrow(t_1, -i\tau), \\ -i\partial_{t_2}G^\uparrow(-i\tau, t_2) &= G^\uparrow(-i\tau, t_2)h^{\text{HF}}(t_2) + I^\uparrow(-i\tau, t_2), \\ i\partial_{t_1}G^\lessgtr(t_1, t_2) &= h^{\text{HF}}(t)G^\lessgtr(t_1, t_2) + I_1^\lessgtr(t_1, t_2), \\ -i\partial_{t_2}G^\lessgtr(t_1, t_2) &= G^\lessgtr(t_1, t_2)h^{\text{HF}}(t_2) + I_2^\lessgtr(t_1, t_2), \end{aligned} \quad (23)$$

with the so-called collision integrals being given by

$$\begin{aligned} I_1^\lessgtr(t_1, t_2) &= \int_0^{t_1} d\bar{t} \Sigma^{\text{R}}(t_1, \bar{t})G^\lessgtr(\bar{t}, t_2) + \int_0^{t_2} d\bar{t} \Sigma^\lessgtr(t_1, \bar{t})G^{\text{A}}(\bar{t}, t_2) - i \int_0^\beta d\bar{\tau} \Sigma^\uparrow(t_1, -i\bar{\tau})G^\uparrow(-i\bar{\tau}, t_2) \\ I_2^\lessgtr(t_1, t_2) &= \int_0^{t_1} d\bar{t} G^{\text{R}}(t_1, \bar{t})\Sigma^\lessgtr(\bar{t}, t_2) + \int_0^{t_2} d\bar{t} G^\lessgtr(t_1, \bar{t})\Sigma^{\text{A}}(\bar{t}, t_2) - i \int_0^\beta d\bar{\tau} G^\uparrow(t_1, -i\bar{\tau})\Sigma^\uparrow(-i\bar{\tau}, t_2) \\ I^\uparrow(t_1, -i\tau) &= \int_0^{t_1} d\bar{t} \Sigma^{\text{R}}(t_1, \bar{t})G^\uparrow(\bar{t}, -i\tau) + \int_0^\beta d\bar{\tau} \Sigma^\uparrow(t_1, -i\bar{\tau})G^M(\bar{\tau} - \tau), \\ I^\uparrow(-i\tau, t_1) &= \int_0^{t_1} d\bar{t} G^\uparrow(-i\tau, \bar{t})\Sigma^{\text{A}}(\bar{t}, t) + \int_0^\beta d\bar{\tau} G^M(\tau - \bar{\tau})\Sigma^\uparrow(-i\bar{\tau}, t_1). \end{aligned} \quad (24)$$

Here the retarded/advanced Green's function  $G^{\text{R/A}}$  and self energy  $\Sigma^{\text{R/A}}$  are functions of  $G^\lessgtr$ . In the above equations, the self energy  $\Sigma(t_1, t_2)$  includes only correlation terms, while the Hartree-Fock contribution is included in  $h^{\text{HF}}(t)$ . The first equation in (23) describes the role of the initial correlations in the propagation of the NEGF. The remaining equations describe the propagation of the two-time particle and hole propagator after leaving equilibrium.

The two-time nature of the KBEs combined with the various collision integrals means the cost of solving these equations scales cubically in the number of time steps. Several approaches have been employed to circumvent the difficulty of performing long NEGF time evolutions. This includes extrapolation of trajectories from a short snapshot of the initial dynamics as well reducing cost through stochastic compression of matrix contractions[15–17]. Another approach is through direct approximation of the full KBEs. The most popular of these approximation schemes is known as the Hartree-Fock generalized Kadanoff-Baym ansatz (HF-GKBA). In the following section, we will introduce the HF-GKBA.

*Implementation details* The KBEs are solved using the NESSi simulation library[18] using a time step of  $dt = .025$  and an inverse temperature  $\beta = 20$ . This value of  $\beta$  was chosen by converging the dynamics with respect to  $\beta$ , so that this effectively is a zero temperature simulation.

#### D. The Generalized Kadanoff-Baym Ansatz

Now we will discuss a commonly used approximation to the Kadanoff-Baym equations, known as the Hartree-Fock generalized Kadanoff-Baym ansatz. Unlike the KBEs, the HF-GKBA does not prepare initial correlations through the contour integration but rather through other means such as adiabatic switching[19, 20]. For this reason only the KBEs with real time arguments are considered in the derivation of the GKBA. The equation of motion for the time-diagonal Green's function can be derived by combining the final two equations in equation (23),

$$i\partial_t G^<(t, t) = [h^{\text{HF}}(t), G^<(t, t)] + I_1^<(t, t) - I_2^<(t, t) \quad (25)$$

with

$$\begin{aligned} I_1^\lessgtr(t_1, t_2) &= \int_0^{t_1} d\bar{t} \Sigma^{\text{R}}(t_1, \bar{t})G^\lessgtr(\bar{t}, t_2) + \int_0^{t_2} d\bar{t} \Sigma^\lessgtr(t_1, \bar{t})G^{\text{A}}(\bar{t}, t_2) \\ I_2^\lessgtr(t_1, t_2) &= \int_0^{t_1} d\bar{t} G^{\text{R}}(t_1, \bar{t})\Sigma^\lessgtr(\bar{t}, t_2) + \int_0^{t_2} d\bar{t} G^\lessgtr(t_1, \bar{t})\Sigma^{\text{A}}(\bar{t}, t_2). \end{aligned} \quad (26)$$

This form of the collision integrals assumes the state at  $t = 0$  has already been prepared in the correlated ground state. We note that now the time arguments lie strictly on the real-time axis.

The HF-GKBA is derived directly from the KBE and can be summarized in the following equations[21],

$$\begin{aligned} G^{\lessgtr}(t_1, t_2) &= iG^R(t_1, t_2)G^{\lessgtr}(t_2, t_2) - iG^{\lessgtr}(t_1, t_1)G^A(t_1, t_2), \\ G^{R,A}(t_1, t_2) &= \pm\Theta[\pm(t_1 - t_2)]T\{e^{-i\int_{t_2}^{t_1} h^{\text{HF}}(t)dt}\}. \end{aligned} \quad (27)$$

In other words, at each time step only equation (25) is explicitly evaluated. Equation (27) is then used to reconstruct the time off-diagonal components.

Apart from those approximations made to the self energy, which HF-GKBA and KBE share, two additional approximations are made in the derivation of HF-GKBA. The first involves neglecting certain integrals that account for time non-local memory effects. These terms appear in the expression for reconstructing  $G^{\lessgtr}(t, t')$ . Once dropped, one is left with the first expression in equation (27). With no further approximation, this ansatz for the time off-diagonal components of  $G^{\lessgtr}(t, t')$  is referred to as the generalized Kadanoff-Baym ansatz(GKBA)[22]. We direct the reader to[] for more details on this approximation. The HF-GKBA involves a further approximation where the full  $G^{R/A}(t, t')$  are replaced by the retarded and advanced Hartree-Fock propagator. Notably, the HF-GKBA leaves important quantities such as energy and particle number conserved as well as retaining causal time evolution.

Recently a linear time scaling[ $\sim O(N_t)$ ] implementation of the HF-GKBA has been achieved, opening the door for long-time evolution of NEGFs[23]. The method removes the explicit appearance of integrals in equation (26) from the differential equation for  $G^<(t)$  by expressing them in terms of the correlated part of the equal time two-particle GF  $\mathcal{G}(t)$ . Within this formulation  $\mathcal{G}(t)$  is propagated simultaneously with  $G^<(t)$  using an expression analogous to equation (25).

The exact equation of motion for  $\mathcal{G}(t)$  depends on the self energy approximation used. In this work we use the  $GW$  self-energy, in whihc case

For the  $GW$  self energy, the equations of motion for  $G^<(t)$  and  $\mathcal{G}(t)$  in the orbital basis are given below[24].

$$\begin{aligned} i\partial_t G_{ij}^<(t) &= [h^{\text{HF}}(t), G^<(t)]_{ij} + [I + I^\dagger]_{ij}(t) \\ i\partial_t \mathcal{G}_{ijkl}(t) &= [h^{(2),\text{HF}}(t), \mathcal{G}(t)]_{ijkl} + \Psi_{ijkl}(t) + \Pi_{ijkl} - \Pi_{lkji}^*. \end{aligned} \quad (28)$$

Above, the following definitions are made,

$$\begin{aligned} h_{ij}^{\text{HF}}(t) &= h_{ij}^{(0)}(t) - i \sum_{kl} [2w_{ikjl}(t) - w_{iklj}(t)]G_{kl}^<(t), \\ I_{ij}(t) &= -i \sum_{klp} w_{iklp}(t)\mathcal{G}_{lpjk}(t), \\ h_{ijkl}^{(2),\text{HF}}(t) &= \delta_{jl}h_{ik}^{\text{HF}}(t) + \delta_{ik}h_{jl}^{\text{HF}}(t), \\ \Psi_{ijkl} &= \sum_{pqrs} [w_{pqrs}(t) - w_{pqsr}(t)] \times \left[ G_{ip}^>(t)G_{rk}^<(t)G_{jq}^>(t)G_{sl}^<(t) - G_{ip}^<(t)G_{rk}^>(t)G_{jq}^<(t)G_{sl}^>(t) \right], \\ \Pi_{ijkl} &= \sum_{pqrs} w_{rqsp} [G_{jr}^>G_{sl}^< - G_{jr}^<G_{sl}^>] \mathcal{G}_{ipkq} \end{aligned} \quad (29)$$

Here  $h^{(0)}(t)$  is the single particle Hamiltonian and  $w_{ijkl}(t)$  is the two-body interaction matrix. The time dependence given to  $w_{ijkl}$  is to allow for adiabatic switching for preparation of the initial state. The tensor  $\Psi_{ijkl}$  accounts for pair correlations built up due to two-particle scattering events and  $\Pi_{ijkl}$  accounts for polarization effects[23].

*Implementation details:* The TD-HF and HF-GKBA equations of motion are solved with the 4th order Runge-Kutta algorithm using a time step of  $dt = 0.02$ . The TD-HF calculation is the special case of  $\mathcal{G}(t) = 0$  in equation (28).

## II. ADDITIONAL RESULTS

### A. Natural populations as a measure of correlation

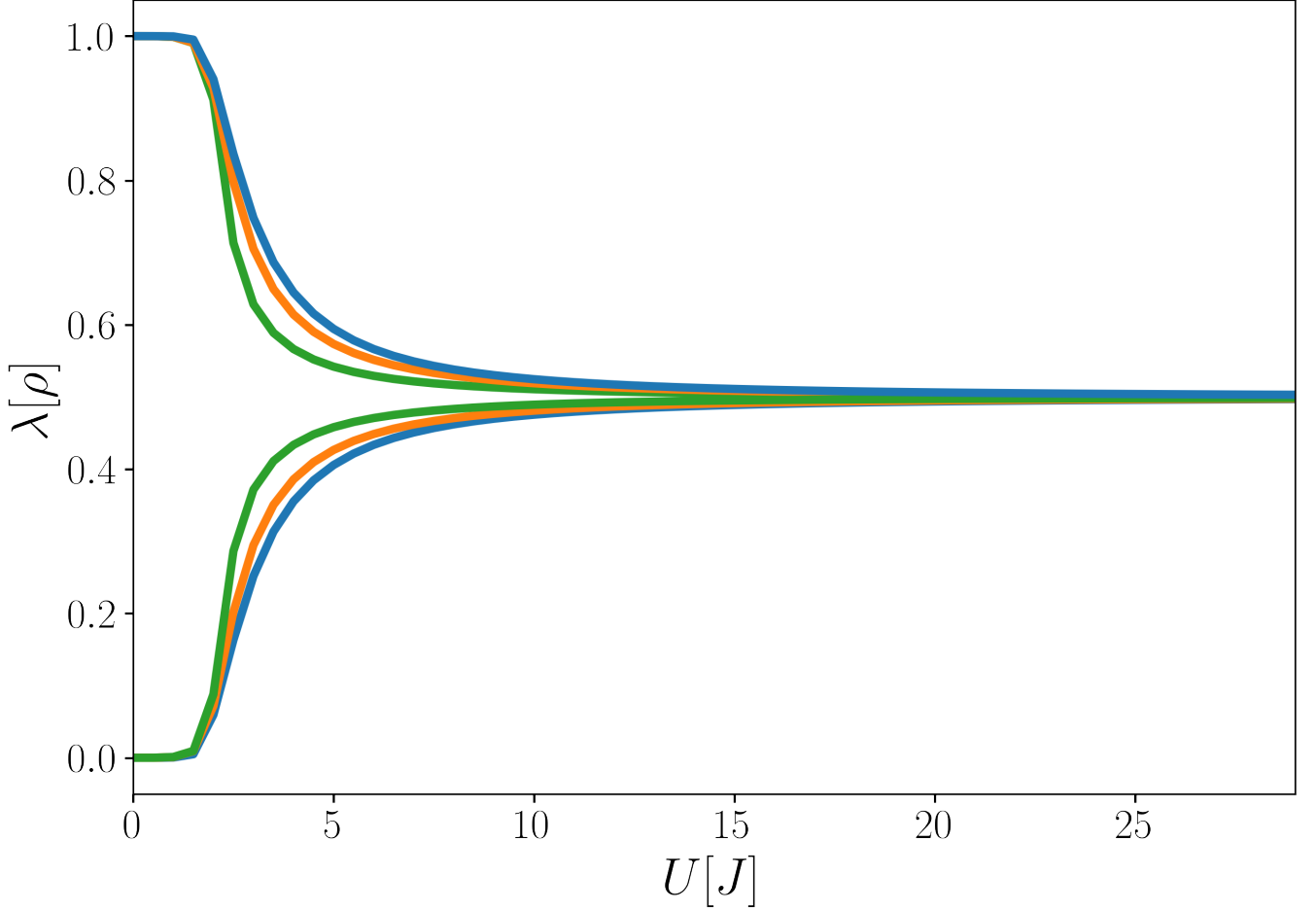


FIG. S3: Example showing the natural occupations as a function of  $U$  for the model given in equation (6) in the main text with  $N_s = 6$ . This helps demonstrate the link between the natural occupations and strong interactions or correlations. In the limit  $U \rightarrow \infty$  the natural occupations approach 0.5. In the main text we look at the evolution of the natural occupations as a measure of the effect of driving on the correlations in the system, there we see that for large field strengths the natural occupations also approach 0.5

### B. Effects of long range interactions

In Fig. S4 we show a set of results similar to those shown in Fig. 2 a)-d) in the main text for a model including long range Coulomb interactions. The explicit Hamiltonian is expressed as,

$$\mathcal{H} = -J \sum_{\langle i,j \rangle \sigma} c_{i\sigma}^\dagger c_{j\sigma} + U \sum_i n_{i\uparrow} n_{i\downarrow} + \gamma U \sum_{ij} \frac{n_i n_j}{|i-j|} + V \sum_i (-1)^i n_i + \sum_{ij} h_{ij}^{\text{N,E}} c_i^\dagger c_j. \quad (30)$$

For the TD-CC results, at low  $E$  values, we see the same excellent agreement as in the case of onsite interactions only. The trend is similar as  $E$  is increased and eventually the TD-CC becomes unstable as before. As has been observed previously[15] the GKBA result improves for lower  $E$  in this long range interacting model. We attribute this to the fact that the  $GW$  self-energy is a more appropriate choice of self-energy in the long range interacting model, since this model will have a larger screening due to the increased interactions. Increasing  $E$  we see a similar trend as before, specifically the HF-GKBA result deviates more from the benchmark result, however is actually able to capture the asymptotic behavior of the TD-CI quite well for high  $E$ .

Results for the KBEs are not included here. The cost of the KBEs with the  $GW$  self-energy becomes too high when we can not take advantage of the onsite only interactions. Judging by previous studies[25] we expect the KBE results to behave very similarly to the HF-GKBA results, with the possibility of additional damping effects being present.

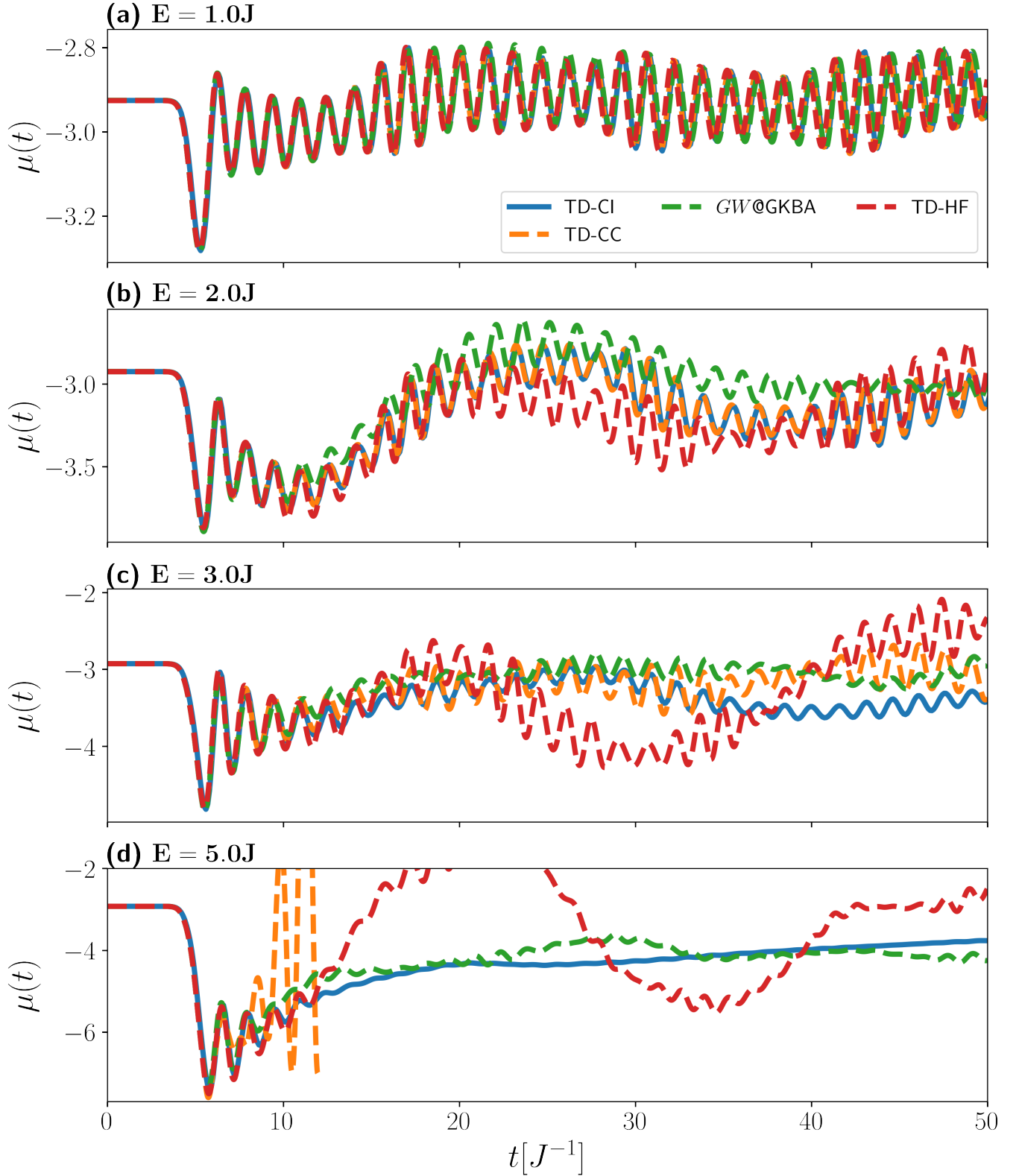


FIG. S4: Dynamics for the system described in equation (30) for different values of the electric field strength  $E$ . a)  $E = 1.0J$ , b)  $2.0J$ , c)  $4.0J$ , d)  $5.0J$ . The model now includes long range Coulomb interactions of the form  $\frac{\gamma U n_i n_j}{|i-j|}$  with  $U = 1.0J$  and  $\gamma = 0.5$



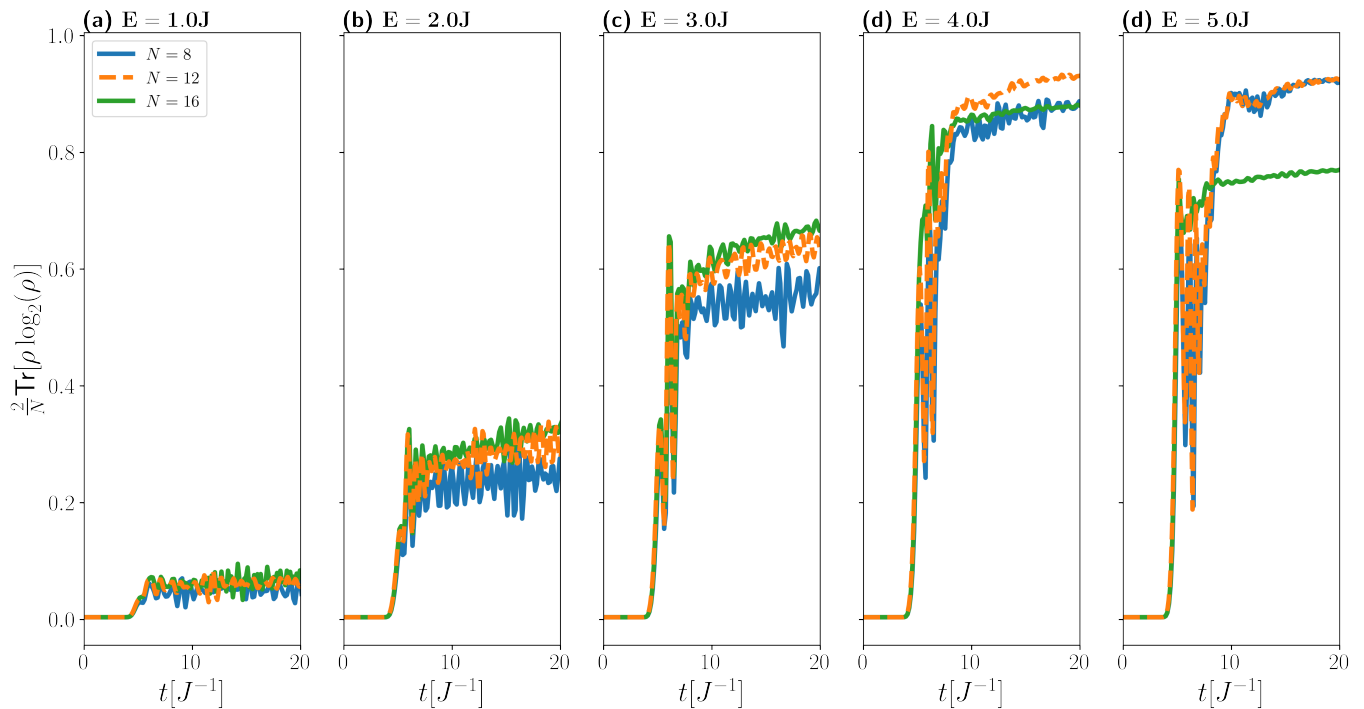


FIG. S5: Von-neumann entropy evaluated with TD-CI for system sizes  $N_s = 8, 12$  and  $16$  with onsite interactions. The system is perturbed from its ground state by the pulse in equation (7) in the main text. Each panel corresponds to a different value of the external field strength  $E$ . a)  $E = 1.0J$ , b)  $E = 2.0J$ , c)  $E = 3.0J$ , d)  $E = 4.0J$ , e)  $E = 5.0J$

### C. Imaginary parts in CC occupation numbers

In the main text, we pointed out that TD-CC, due to its non-Hermitian nature, develops imaginary or unphysical parts in physical observables. In Fig. S6, as a prototypical example, we plot the imaginary parts for the TD=CC expectation value for electron density on the first site in Hubbard lattice. As the strength of the time-dependent perturbation increases, TD-CC results start accumulating increasingly larger imaginary parts in the occupation number. In fact, for  $E = 4J$  and  $E = 5J$ , with such large unphysical components in electron density, the theory is no longer well behaved, and can be deemed a failure. This property, however, makes TD-CC unique as it provides a diagnostic tool to assess its own effectiveness.

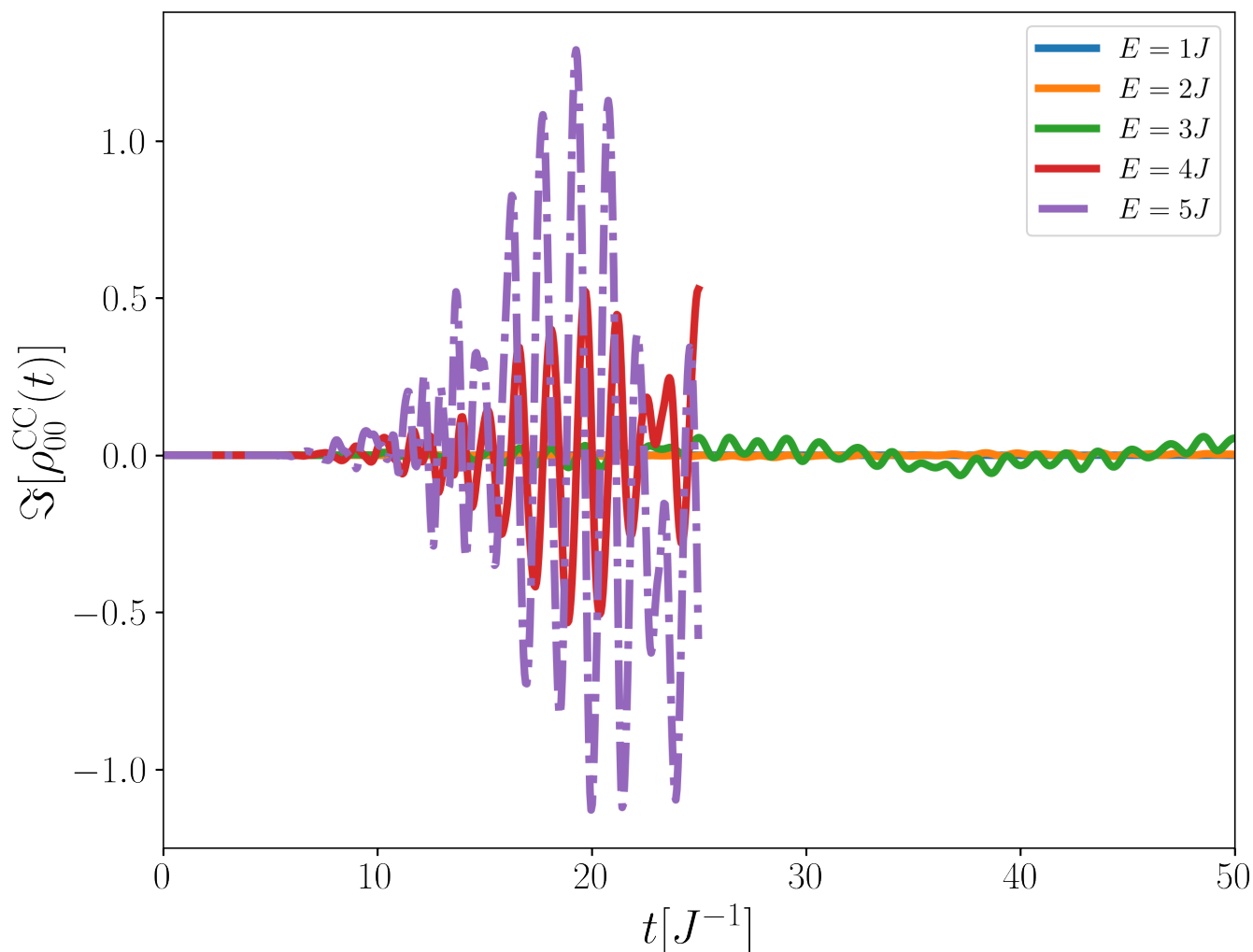


FIG. S6: Imaginary part in occupation number for the first site in the model lattice in equation (7) in the main text, as predicted by time-dependent CCSD for  $N_s = 12$ . Results for different perturbation strength  $E$  show that for large perturbation, TD-CC occupations develop imaginary parts, that increase as we evolve in time. On the other hand, for weak interactions, the imaginary terms are well behaved and can be disregarded.

- 
- [1] T. J. Park and J. C. Light, Unitary quantum time evolution by iterative Lanczos reduction, *J. Chem. Phys.* **85**, 5870 (1986).
- [2] N. Mohankumar and S. M. Auerbach, On time-step bounds in unitary quantum evolution using the lanczos method, *Computer Physics Communications* **175**, 473 (2006).
- [3] Q. Sun, T. C. Berkelbach, N. S. Blunt, G. H. Booth, S. Guo, Z. Li, J. Liu, J. D. McClain, E. R. Sayfutyarova, S. Sharma, S. Wouters, and G. K.-L. Chan, PySCF: the Python-based simulations of chemistry framework, *WIREs Computational Molecular Science* **8**, e1340 (2018).
- [4] Q. Sun, X. Zhang, S. Banerjee, P. Bao, M. Barbry, N. S. Blunt, N. A. Bogdanov, G. H. Booth, J. Chen, Z.-H. Cui, J. J. Eriksen, Y. Gao, S. Guo, J. Hermann, M. R. Hermes, K. Koh, P. Koval, S. Lehtola, Z. Li, J. Liu, N. Mardirossian, J. D. McClain, M. Motta, B. Mussard, H. Q. Pham, A. Pulkin, W. Purwanto, P. J. Robinson, E. Ronca, E. R. Sayfutyarova, M. Scheurer, H. F. Schurkus, J. E. T. Smith, C. Sun, S.-N. Sun, S. Upadhyay, L. K. Wagner, X. Wang, A. White, J. D. Whitfield, M. J. Williamson, S. Wouters, J. Yang, J. M. Yu, T. Zhu, T. C. Berkelbach, S. Sharma, A. Y. Sokolov, and G. K.-L. Chan, Recent developments in the PySCF program package, *J. Chem. Phys.* **153**, 024109 (2020).
- [5] T. D. Crawford and H. F. Schaefer, An Introduction to Coupled Cluster Theory for Computational Chemists, in *Reviews in Computational Chemistry*, edited by K. B. Lipkowitz and D. B. Boyd (John Wiley & Sons, Inc., 2000) pp. 33–136.
- [6] R. J. Bartlett and M. Musiał, Coupled-cluster theory in quantum chemistry, *Rev. Mod. Phys.* **79**, 291 (2007).

- [7] J. Arponen, Variational principles and linked-cluster expansion for static and dynamic many-body problems, *Annals of Physics* **151**, 311 (1983).
- [8] J. Zhao, *Symbolic solution for computational quantum many-body theory development*, PhD Thesis, Rice University (2018).
- [9] P. N. Brown, G. D. Byrne, and A. C. Hindmarsh, VODE: A Variable-Coefficient ODE Solver, *SIAM J. Sci. and Stat. Comput.* **10**, 1038 (1989).
- [10] P. Virtanen, R. Gommers, T. E. Oliphant, M. Haberland, T. Reddy, D. Cournapeau, E. Burovski, P. Peterson, W. Weckesser, J. Bright, S. J. van der Walt, M. Brett, J. Wilson, K. J. Millman, N. Mayorov, A. R. J. Nelson, E. Jones, R. Kern, E. Larson, C. J. Carey, Í. Polat, Y. Feng, E. W. Moore, J. VanderPlas, D. Laxalde, J. Perktold, R. Cimrman, I. Henriksen, E. A. Quintero, C. R. Harris, A. M. Archibald, A. H. Ribeiro, F. Pedregosa, P. van Mulbregt, and SciPy 1.0 Contributors, SciPy 1.0: Fundamental Algorithms for Scientific Computing in Python, *Nat. Methods* **17**, 261 (2020).
- [11] A. Stan, N. Dahlen, and R. van Leeuwen, Time propagation of the Kadanoff–Baym equations for inhomogeneous systems, *J. Chem. Phys.* **130**, 224101 (2009).
- [12] G. Stefanucci and R. van Leeuwen, *Nonequilibrium Many-Body Theory of Quantum Systems: A Modern Introduction* (Cambridge University Press, 2013).
- [13] L. Kadanoff and G. Baym, *Quantum Statistical Mechanics* (W.A. Benjamin Inc., New York, 1962).
- [14] M. Bonitz, *Quantum Kinetic Theory* (Springer International Publishing Switzerland, 2015).
- [15] C. C. Reeves, J. Yin, Y. Zhu, K. Z. Ibrahim, C. Yang, and V. Vlček, Dynamic mode decomposition for extrapolating nonequilibrium Green’s-function dynamics, *Phys. Rev. B* **107**, 075107 (2023).
- [16] J. Yin, Y.-h. Chan, F. da Jornada, D. Qiu, C. Yang, and S. G. Louie, Analyzing and predicting non-equilibrium many-body dynamics via dynamic mode decomposition, *arXiv preprint arXiv:2107.09635* (2021).
- [17] L. Mejía, J. Yin, D. R. Reichman, R. Baer, C. Yang, and E. Rabani, Stochastic Real-Time Second-Order Green’s Function Theory for Neutral Excitations in Molecules and Nanostructures (2023), *arXiv:2303.06874 [physics.chem-ph]*.
- [18] M. Schüler, D. Golež, Y. Murakami, N. Bittner, A. Herrmann, H. U. Strand, P. Werner, and M. Eckstein, NESSi: The Non-Equilibrium Systems Simulation package, *Computer Physics Communications* **257**, 107484 (2020).
- [19] R. Tuovinen, D. Golež, M. Schüler, P. Werner, M. Eckstein, and M. A. Sentef, Adiabatic Preparation of a Correlated Symmetry-Broken Initial State with the Generalized Kadanoff–Baym Ansatz, *physica status solidi (b)* **256**, 1800469 (2019).
- [20] D. Karlsson, R. van Leeuwen, E. Perfetto, and G. Stefanucci, The generalized Kadanoff–Baym ansatz with initial correlations, *Phys. Rev. B* **98**, 115148 (2018).
- [21] S. Hermanns, K. Balzer, and M. Bonitz, The non-equilibrium Green function approach to inhomogeneous quantum many-body systems using the generalized Kadanoff–Baym ansatz, *Physica Scripta* **T151**, 014036 (2012).
- [22] P. Lipavský, V. Špička, and B. Velický, Generalized Kadanoff–Baym ansatz for deriving quantum transport equations, *Phys. Rev. B* **34**, 6933 (1986).
- [23] J.-P. Joost, N. Schlünzen, and M. Bonitz, G1-G2 scheme: Dramatic acceleration of nonequilibrium Green functions simulations within the Hartree-Fock generalized Kadanoff–Baym ansatz, *Phys. Rev. B* **101**, 245101 (2020).
- [24] N. Schlünzen, J.-P. Joost, and M. Bonitz, Achieving the Scaling Limit for Nonequilibrium Green Functions Simulations, *Phys. Rev. Lett.* **124**, 076601 (2020).
- [25] C. C. Reeves, Y. Zhu, C. Yang, and V. Vlček, Unimportance of memory for the time nonlocal components of the kadanoff-baym equations, *Phys. Rev. B* **108**, 115152 (2023).